Seismic performance of a 12-storey ductile concrete shear wall system designed according to the 2005 *National building code of Canada* and the 2004 Canadian Standard Association standard A23.3

Yannick Boivin and Patrick Paultre

Abstract: This paper presents an assessment of the seismic performance of a ductile concrete core wall used as a seismic force resisting system for a 12-storey concrete office building in Montréal, designed according to the 2005 *National building code of Canada* (NBCC) and the 2004 Canadian Standards Association standard A23.3. The core wall consists of a cantilever wall system in one direction and a coupled wall system in the orthogonal direction. The building is analyzed in the nonlinear regime. The main conclusion from this work is that the capacity design shear envelope for the studied wall structure largely underestimates that predicted, primarily in the cantilever wall direction, and this in turn significantly increases the risk of shear failure. This issue is essentially due to (*i*) an underestimation by the new NBCC spectral response acceleration of the higher mode responses of a reinforced concrete wall structure whose seismic response is dominated by higher modes; and (*ii*) a deficiency in the capacity design method in estimating the wall shear demand on such walls, even when their behavior is lightly inelastic.

Key words: 2005 NBCC, 2004 CSA standard A23.3, ductile concrete cantilever and coupled shear wall systems, seismic design, higher mode effects, seismic shear demand.

Résumé : Cet article présente une évaluation de la performance sismique d'un système de murs de contreventement ductiles utilisé comme système de résistance aux forces sismiques pour un bâtiment de 12 étages en béton armé dimensionné selon le CNBC 2005 et la Norme CSA A23.3 2004, et situé à Montréal. Le système de murs se comporte comme un mur en cantilever dans une direction et comme un mur couplé dans la direction orthogonale. Le bâtiment est analysé dans le régime non-linéaire. La conclusion principale de ce travail est que l'enveloppe de dimensionnement à la capacité en cisaillement sous-estime largement celle prédite, surtout dans la direction du mur en cantilever, et que ceci en retour augmente significativement le risque de rupture par cisaillement. Ce problème est essentiellement causée par (*i*) une sous-estimation par l'accélération spectrale du CNBC des réponses des modes supérieurs de vibration d'un mur en béton armé dont la réponse sismique est dominée par les modes supérieurs; et (*ii*) une déficience de la méthode de dimensionnement à la capacité à estimer la demande en cisaillement sur de tels murs, même lorsque leur comportement est légèrement inélastique.

Mots-clés : CNBC 2005, Norme CSA A23.3 2004, Système de murs de contreventement ductiles en béton armé, Effets dynamiques des modes supérieurs, demande sismique en cisaillement.

[Traduit par la Rédaction]

1. Introduction

Recent Canadian numerical studies (Tremblay et al. 2001; Renaud 2004) suggested that the seismic design strength envelopes for ductile reinforced concrete (RC) shear walls determined in accordance with the requirements of the 1995 edition of the *National building code of Canada* (NRCC 1995) and the capacity design considerations specified in the 1994 edition of Canadian Standards Association (CSA) standard A23.3 for the design of concrete structures (A23.3-94) (CSA 1994) may underestimate the seismic shear and flexural demands on cantilever walls subjected to design-level ground motions. Comparable observations were also reported by Amaris (2002) for similar capacity design considerations, even for ground motion intensities lower than that of the design level. For ductile RC coupled wall systems designed according to the 1995 NBCC and CSA standard A23.3-94, no such issues have been reported in the published literature, except for systems whose shear strength design is based on the tension wall rather than the compression wall (Chaallal and Gauthier 2000) and for systems subjected to seismic events much more severe than that used for

Received 3 October 2008. Revision accepted 21 July 2009. Published on the NRC Research Press Web site at cjce.nrc.ca on 23 January 2010.

Y. Boivin and P. Paultre.[1] Department of Civil Engineering, Université de Sherbrooke 2500, boul. de l'Université, Sherbrooke, QC J1K 2R1, Canada.

Written discussion of this article is welcomed and will be received by the Editor until 31 May 2010.

[1]Corresponding author (e-mail: Patrick.Paultre@USherbrooke.ca).

design (Renaud 2004; White and Ventura 2004). The underestimation issue of the capacity-based seismic design envelopes for flexural and shear strength designs would primarily result from a large underestimation of the dynamic magnification effects due to lateral modes of vibration higher than the fundamental lateral mode.

Although the improvements made to the seismic design provisions of the 2005 edition of the NBCC (NRCC 2005) and the 2004 edition of CSA standard A23.3 (A23.3-04) (CSA 2004) do not specifically address the aforementioned issue, they provide a more rational seismic design approach for ductile RC shear wall systems. Very few published works (Panneton et al. 2006) have studied the seismic performance of such systems resulting from the application of these new design codes. In this regard, this paper presents an assessment of the seismic performance of a ductile RC shear wall system used as a seismic force resisting system (SFRS) for a 12-storey RC building designed and detailed according to the 2005 NBCC and CSA standard A23.3-04.

In this work, some of the new seismic design provisions of the 2005 NBCC and CSA standard A23.3-04 are examined, emphasizing their application for ductile concrete shear wall structures. Insight is also given into how higher mode effects on shear forces in such structures are addressed in these codes and how the capacity design strength envelopes for these structures are determined. The seismic design of the wall system is briefly presented as are the inelastic structural models, analysis parameters, and earthquake inputs used for the seismic performance assessment.

2. Canadian seismic design code provisions

2.1. 2005 *National building code of Canada*

In contrast with previous editions of the NBCC, dynamic analysis is now the default analysis method for seismic design. The traditional equivalent static force procedure can still be used, but only for specific cases. Independently of the design procedure used, a minimum base shear force, V, must be considered in determining the design shear force at the base of the building:

$$[1] \qquad V = \frac{S(T_a)M_v I_E W}{R_d R_o}$$

where $S(T_a)$ is the new design spectral response acceleration, expressed as a ratio of gravitational acceleration, for the fundamental lateral period of vibration, T_a, of the building in the loading direction of interest; M_v is a new factor to account for higher mode effects on base shear; I_E is the earthquake importance factor of the building ($0.8 \le I_E \le 1.5$); W is the seismic weight of the building; R_d is the ductility-related force modification factor ($1.0 \le R_d \le 5.0$); and R_o is a new overstrength-related force modification factor ($1.0 \le R_o \le 1.7$) that accounts for the dependable portion of reserve strength in the SFRS. The design spectral acceleration, $S(T)$, is determined as

$$[2] \qquad S(T) = F_a S_a(T) \text{ or } F_v S_a(T)$$

where $S_a(T)$ is the 5% damped spectral response acceleration at period T determined for a probability of exceedance of 2% in 50 years at a median confidence level; and F_a and F_v are new acceleration- and velocity-based site coefficients, respectively. Both site coefficients represent the amplification of seismic motions due to ground conditions. $S_a(T)$ is a uniform hazard spectrum (UHS) where the spectral accelerations at different periods are calculated at the same probability of exceedance for a specific geographical location. The $S_a(T)$ values given in the 2005 NBCC were determined for the reference ground condition of very dense soil or soft rock. The fundamental lateral period of vibration, T_a, of the building can be determined either with the NBCC empirical relation for the SFRS of interest or from established methods of mechanics using a structural model that complies with NBCC requirements. For shear wall structures, T_a determined from the latter methods cannot be taken greater than 2.0 times that determined with the empirical relation, which is now $0.05(h_n)^{3/4}$, where h_n is the building height above the base in metres, and n is the number of storeys. This limitation is to ensure that computed T_a values will not be much greater than those measured in actual buildings, as structural models tend to be more flexible than the actual building.

The new M_v factor in eq. [1] accounts for the dynamic magnification of base shear due to higher modes. The derivation of this factor can be found in Humar and Mahgoub (2003). The M_v values specified in the 2005 NBCC are a function of the type of SFRS, T_a, and the shape of the spectral response acceleration, $S_a(T)$. Table 1 gives the M_v values specified in the 2005 NBCC for shear walls. A ratio $S_a(0.2)/S_a(2.0) < 8.0$ is typical for the western Canadian regions, and a ratio $S_a(0.2)/S_a(2.0) \ge 8.0$ is typical for the eastern Canadian regions. For $T_a > 1.0$, Table 1 indicates that the dynamic magnification of base shear due to higher modes is more significant for eastern regions than for western regions and increases with increasing T_a.

It is important to note that, although both factors were determined to amplify the shear forces produced by the common code-specified static lateral force distribution, the M_v factor is not equivalent to the dynamic shear magnification factor, ω_v, specified in the New Zealand concrete design standard (NZS 1995) for the shear strength design of ductile concrete shear wall structures. The M_v factor only takes into account the magnification of base shear due to elastic effects of higher modes, whereas ω_v accounts for the magnification of shear forces due to inelastic effects of higher modes (Blakeley et al. 1975). In addition, it is of interest to note that, unlike M_v values, ω_v values depend only on the fundamental lateral period of vibration (number of storeys) of the building: $\omega_v = 0.9 + n/10$ for buildings up to six storeys and $1.3 + n/30$, to a maximum of 1.8, for taller buildings, where n is the number of storeys. As noted by Priestley (2003), the current form of ω_v is deficient in capturing all significant causative parameters. Consequently, various numerical works (Bachmann and Linde 1995; Amaris 2002; Panneton et al. 2006) suggest that the actual inelastic dynamic shear magnification in cantilever walls can be much larger than that predicted by ω_v. However, experimental investigations on this high magnification issue are needed, since the limited experimental work (Eberhard and Sozen 1993) published so far does not report such large shear magnifications.

2.2. CSA standard A23.3-04

As linear analysis is generally used to predict earthquake

Table 1. Values specified in the 2005 NBCC for shear walls of the factor M_v to account for higher mode effects on base shear.

$S_a(0.2)/S_a(2.0)$	Type of SFRS	$T_a \leq 1.0$	$T_a \geq 2.0$
<8.0	Coupled wall[a]	1.0	1.0
<8.0	Shear wall	1.0	1.2
≥8.0	Coupled wall	1.0	1.2
≥8.0	Shear wall	1.0	2.5

[a]Coupled wall is a shear wall system with coupling beams in which at least 66% of the base overturning moment resisted by the entire wall system is carried by the earthquake-induced axial forces in walls resulting from shear in the coupling beams.

design actions, the seismic design provisions of CSA standard A23.3-04 (CSA 2004) for ductile RC walls are based on capacity design principles. These provisions are mainly for wall structures that are substantially uniform and regular in strength and stiffness over the full height of the building.

2.2.1. Flexural strength design

For ductile RC walls designed for a single plastic hinge at the wall base, CSA standard A23.3-04 provides new capacity design provisions to prevent unexpected flexural yielding above the assumed base hinging region, which is taken to be at least 1.5 times the wall length, l_w, in the direction under consideration (Fig. 1). From these provisions, a capacity moment envelope can be determined, corresponding to the development of the factored moment resistance (M_r) of the wall section over the assumed base hinging region. Note that M_r is calculated with factored material strengths, which are lower than their specified values. The capacity moment envelope is obtained by amplifying the NBCC design (factored) overturning moments for the wall, obtained from linear analysis, by the ratio of M_r to the factored moment, M_f, both calculated at the top of the assumed plastic hinge region, as shown in Fig. 1. The factored moment resistance of the wall above the assumed hinging region must be set to match or exceed the resulting capacity moment envelope.

Previously, the *Explanatory notes on CSA standard A23.3-94* (CAC 1995) suggested that the capacity moment envelope be taken as a probable moment envelope varying linearly from the top of the assumed hinging region to the top of the wall, as illustrated in Fig. 1. This envelope assumes a first-mode lateral behavior of walls after plastic hinge formation at the wall base. The probable moment resistance, M_p, of the wall above the hinging region had to match or exceed this linear envelope. However, recent numerical works (Tremblay et al. 2001; Renaud 2004) suggested that this approach might not prevent the formation of unintended plastic hinges above the base of multistorey walls due to higher mode effects. Note that M_p is calculated with a concrete compressive strength (f'_c) at its specified value and an equivalent steel yield stress of 1.25 times its specified value (f_y).

2.2.2. Shear strength design

To satisfy the shear strength requirements of CSA standard A23.3-04, the factored shear resistance, V_r, of a ductile RC shear wall must not be less than the shear corresponding to the development of the probable moment capacity of the wall at its plastic hinge locations, accounting for the magnification of shear forces due to inelastic effects of higher modes. CSA standard A23.3-04 limits this probable envelope to a shear resulting from the NBCC design load combinations, which include earthquakes with load effects calculated using $R_dR_o = 1.0$. It is of interest to note that CSA standard A23.3-04 does not prescribe any method to determine the probable shear envelope, nor any method to account for the inelastic dynamic shear magnification effect. For a single-base-hinge design of walls, the *Explanatory notes on CSA standard A23.3-04* (CAC 2006*a*) suggest, as in the previous edition, that the probable shear envelope, V_p, on walls be estimated by amplifying the NBCC design shear force envelope, V_f, for the wall, obtained from linear analysis, as follows:

$$[3] \qquad V_p = \gamma_p V_f = \left(\frac{M_p}{M_f}\right)_{base} V_f$$

where γ_p is the probable wall overstrength factor, and the ratio M_p/M_f is calculated at the wall base. CAC (2006*a*), however, indicates that no Canadian method is available at this time to account for the magnification of shear forces due to inelastic effects of higher modes. Even the adaptation of New Zealand's dynamic shear magnification factor ω_v to Canadian codes suggested in CAC (1995) is no longer considered in the new edition (CAC 2006*a*). This appears to be a major issue because recent studies (Tremblay et al. 2001; Renaud 2004; Panneton et al. 2006) suggest that V_p (eq. [3]) considerably underestimates the shear demand on ductile RC walls subjected to design-level ground motions.

For a single-base-hinge design of ductile walls, CSA standard A23.3-04 now provides an additional requirement for the shear strength design at all elevations above the assumed plastic hinge height of $1.5l_w$ (Fig. 1). At each section above this height, the factored shear forces, V_f, must be scaled up by the same ratio M_r/M_f used to determine the capacity moment envelope above the hinging region. V_r of the wall must not be less than the maximum of the resulting shear envelope and the probable shear envelope, V_p, above the hinging region.

Fig. 1. Capacity design moment envelopes for ductile RC walls.

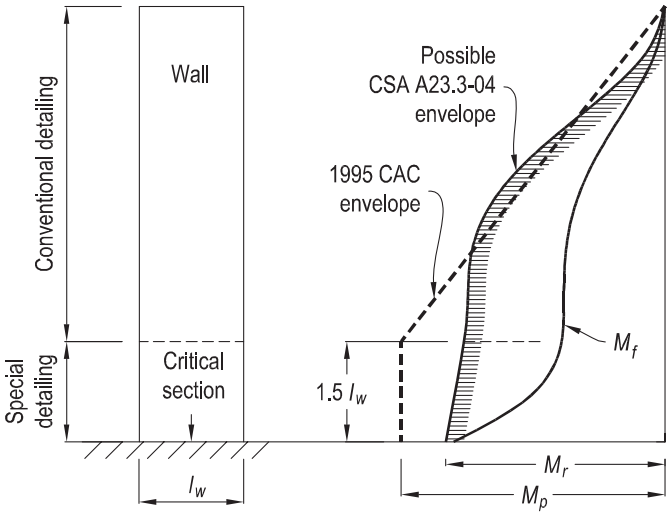

3. Studied building

3.1. Description

This research project studied a 12-storey RC office building located in Montréal and founded on soft rock, which is the reference ground condition (class C) in the 2005 NBCC. The structural configuration and dimensions of the building structure are shown in Fig. 2. The structure is made of normal-density concrete and steel reinforcement with specified strengths f'_c = 30 MPa and f_y = 400 MPa. The SFRS is a central elevator core wall bracing a flat slab–column system with spandrel beams located along the exterior edges of each floor. The core wall extends one storey above the roof of the building, forming an elevator penthouse on the 13th floor. The core wall cross section measures 6 m × 8 m, centre to centre, and its thickness is 400 mm, for stability considerations, over the entire height of the wall. The core wall is composed of two C-shaped walls connected at the level of each floor by two 1 m deep coupling beams with a span to depth ratio of 1.8. This configuration results in a coupled wall system in the east–west direction and a cantilever wall system in the north–south direction. It is noted that the building is very similar to the sample building in the 2006 edition of the Canadian *Concrete design handbook* (CAC 2006*b*). Herein, however, coupling beams are less slender, resulting in a more heavily coupled wall system. The dimensions of the other structural components of the building and the complete design and detailing of the building structure can be found in Boivin (2006). Only a brief overview of the seismic design of the core wall is presented in the following sections.

3.2. Seismic design according to the 2005 NBCC

The core wall was designed to resist 100% of the earthquake loads and their effects, as required by the 2005 NBCC. An R_d value of 3.5 was used for the cantilever wall direction and 4.0 for the coupled wall direction, as the coupled wall system can be considered fully coupled (degree of coupling greater than 66%).

The NBCC earthquake design loads were determined from a linear modal response spectrum analysis using the design acceleration response spectrum, $S(T)$, for Montréal, with site coefficients $F_a = F_v = 1.0$ (soft rock). The dynamic analysis showed that the building structure was torsionally sensitive, and hence irregular, as defined by the 2005 NBCC. Consequently, the code-specified static procedure was not permitted for seismic design. The total lateral responses in each principal direction were obtained by combining the spectral responses of the first three lateral modes with the SRSS (square root of the sum of the squares) method.

Table 2 gives the parameters used to calculate V, V_{dyn} (which is the base shear obtained from linear dynamic analysis), and the resulting NBCC design base loads for the building in each principal direction. The NBCC design base shears are equal to the larger of V and V_{dyn}, as the building structure is irregular in torsion. As permitted, the NBCC earthquake design loads are based on T_a computed from modal analysis. The T_a values are 1.74 s for the cantilever wall direction and 1.41 s for the coupled wall direction. These values do not exceed the NBCC-specified limit of two times the T_a value calculated with the NBCC empirical relation, which gives

Fig. 2. Reinforced concrete (RC) core wall building.

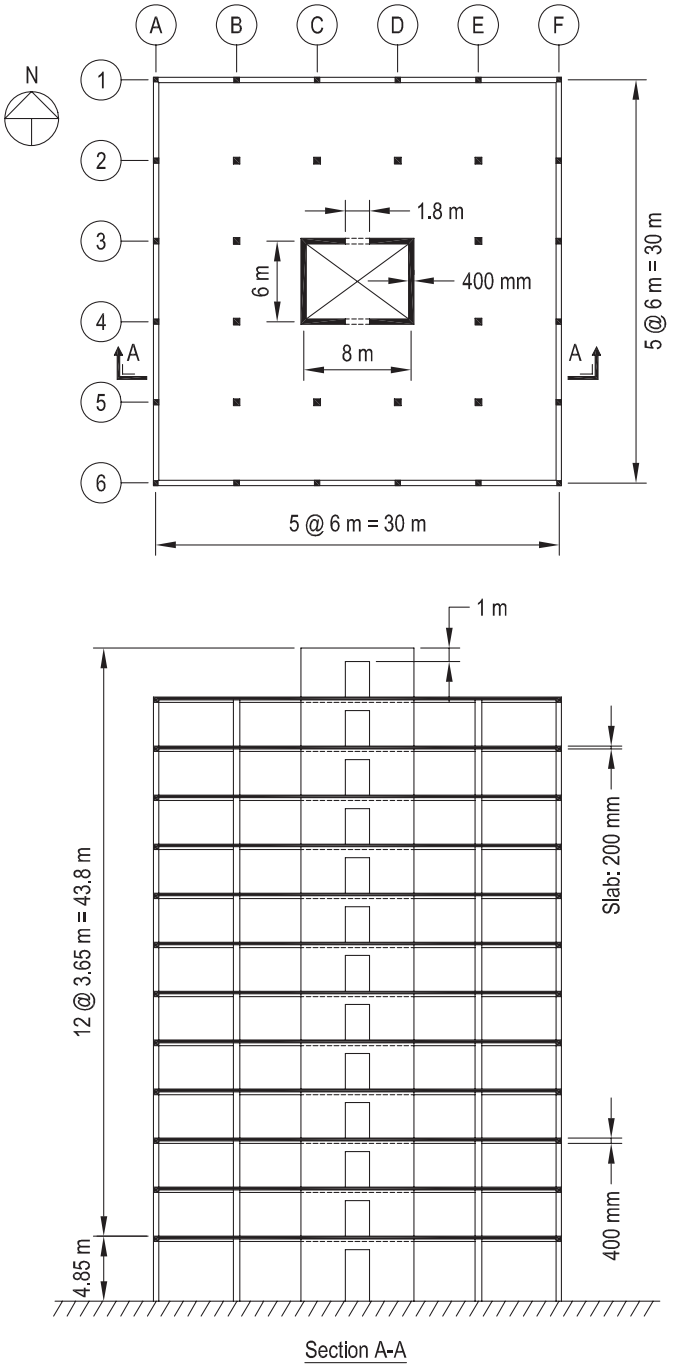

$T_a = 0.87s$. The use of the computed T_a values rather than the empirical one has significantly reduced the earthquake design loads, as indicated in Table 2. This is due, in part, to the design spectrum shape for Montréal, where the $S(T_a)$ values are reduced by about 50% and 60% as the period values increase from 0.87 to 1.41 and 1.74 s, respectively.

The estimated overall and interstorey drifts of the building structure at design displacements, including the inelastic part, are low. In each principal direction, the overall building drift and the maximum interstorey drift for all storeys are not greater than 0.30%, which is significantly less than the NBCC limit of 2.5% for this building.

Table 2. NBCC 2005 earthquake design loads for the studied building.

Seismic loading direction	Type of SFRS[a]	Parameters used to calculate V (eq. [1])						Base shear		NBCC design base forces			Force reduction (%)
		T_a (s)	$S(T_a)$ (g)	M_v	R_d	R_o	I_E	W (kN)	V (kN)	V_{dyn} (kN)	V_{do} (kN)	M_{do} (kN·m)	T_{do} (kN·m)	
E–W	DFCW	0.87[b]	0.19	1.00	4.0	1.7	1.0	86 626	2452	1760	2452	44 604	7455	Ref.
E–W	DFCW	1.41[c]	0.10	1.04	4.0	1.7	1.0	86 626	1355	1760	**1760**	**32 017**	**5351**	–28.2
N–S	DCW	0.87[b]	0.19	1.00	3.5	1.6	1.0	86 626	2978	2062	2978	41 958	9053	Ref.
N–S	DCW	1.74[c]	0.07	1.74	3.5	1.6	1.0	86 626	1938	2062	**2062**	**29 057**	**6269**	–30.8

Note: Force values in bold are those used for design. V_{dyn}, factored base shear obtained from SRSS; V_{do}, M_{do}, and T_{do}, shear force, overturning moment, and (accidental) torsional moment, respectively. The NBCC base overturning modification factor J is 0.93 (0.87 s) and 0.82 (1.41 s) for DFCW and 0.85 (0.87 s) and 0.51 (1.74 s) for DCW.

[a]DCW, ductile cantilever wall; DFCW, ductile fully coupled wall.

[b]Period calculated with the NBCC empirical relation.

[c]Period computed from modal analysis.

Figure 3 illustrates the contribution of higher lateral modes on the NBCC earthquake design force profiles over the entire height of the building. It indicates that higher mode effects play a major role in the seismic forces applied to the studied building structure, especially in the north–south direction.

3.3. Seismic design according to CSA standard A23.3-04

Because of the uniform structural configuration of the core wall, a single-base-hinge design is adopted for the walls. In the coupled wall direction, the coupling beams are designed to yield prior to the walls under a pushover loading. The resulting detailing characteristics of the core wall are as follows.

(1) The lower first three storeys of the walls are detailed as a plastic hinge region. This height is governed by the wall length l_w in the north–south direction and is higher than the required minimum height of $1.5l_w$.
(2) The flexural (vertical) reinforcement in the walls is governed by the required minimum reinforcement over the entire height of the core wall.
(3) The required minimum flexural reinforcement in the assumed plastic hinge region ($1.5l_w$) is extended along the height of the wall up to storey 9, inclusive. Above this storey, there is a curtailment of the flexural reinforcement. This curtailment is based on the factored moment resistance (M_r) of a C-shaped wall matching or exceeding the capacity design moment envelope prescribed by CSA standard A23.3-04, as illustrated in Fig. 4*a*.
(4) The shear (horizontal) reinforcement in the assumed base hinging region ($1.5l_w$) is governed by the shear strength required to develop the probable flexural capacity (V_p, eq. [3]) of a C-shaped wall in the north–south direction. The plastic hinge detailing for shear is extended up to storey 5, inclusive, to satisfy the shear strength requirement above the assumed hinging region. Above storey 5, the shear reinforcement in the walls is governed by the required minimum reinforcement, as shown in Fig. 4*b*.
(5) Diagonal reinforcement is provided in the coupling beams. The beam reinforcement yielding strength matches as closely as possible the design beam shear envelope after up to 20% vertical redistribution was applied between beams, as suggested in CAC (2006*a*).

As shown in Fig. 4*a* for the north–south direction, the core wall has substantial flexural overstrength compared with that of the NBCC design envelope determined with either permitted values of T_a. The wall overstrength factor, γ_w, which is defined as the ratio of nominal moment resistance M_n to the factored moment M_f at the base of the wall system, is about 3.6 for each principal direction. Note that γ_w would be about 2.5 if M_f is based on the empirical T_a value of 0.87 s. This large overstrength is due to the excess strength arising from the required minimum reinforcement. This is typical for core walls located in moderate seismic regions such as Montréal but may not be the case in high seismic regions such as Vancouver, particularly for tall buildings for which the minimum base shear cutoff at a period of 2 s usually applies. Despite the large flexural overstrength of the walls, the requirement for the sliding shear resistance at the wall base is barely satisfied, assuming that the construction joint is intentionally roughened. Note that

Fig. 3. NBCC seismic design force profiles over building height in both directions: (*a*) shear force; (*b*) overturning moment.

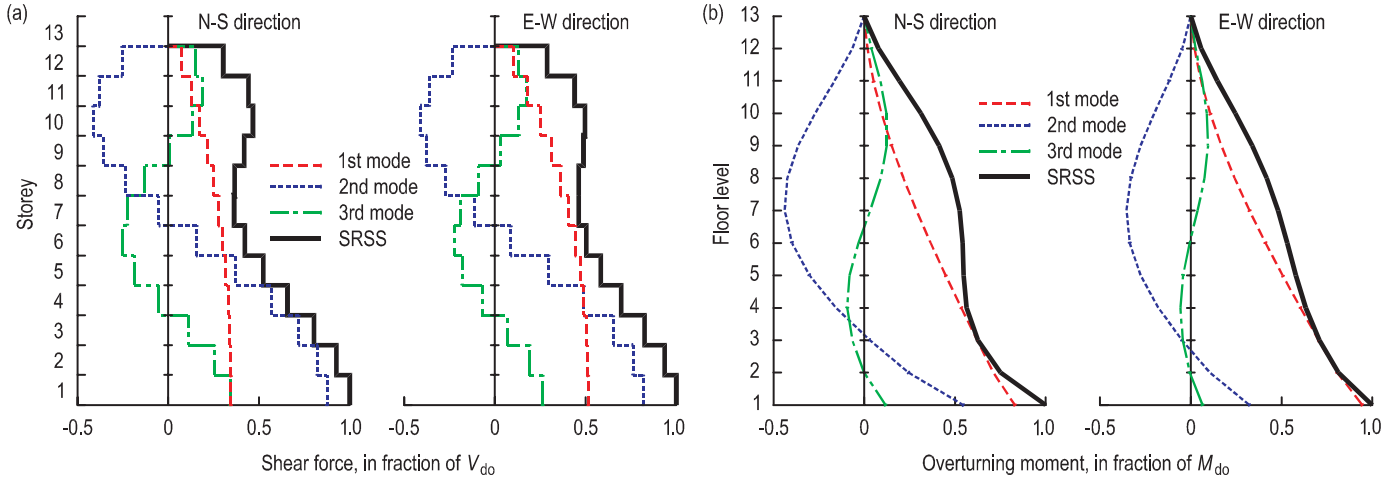

Fig. 4. Capacity design of a C-shaped wall in the north–south direction according to CSA standard A23.3-04: (*a*) in flexure; (*b*) in shear.

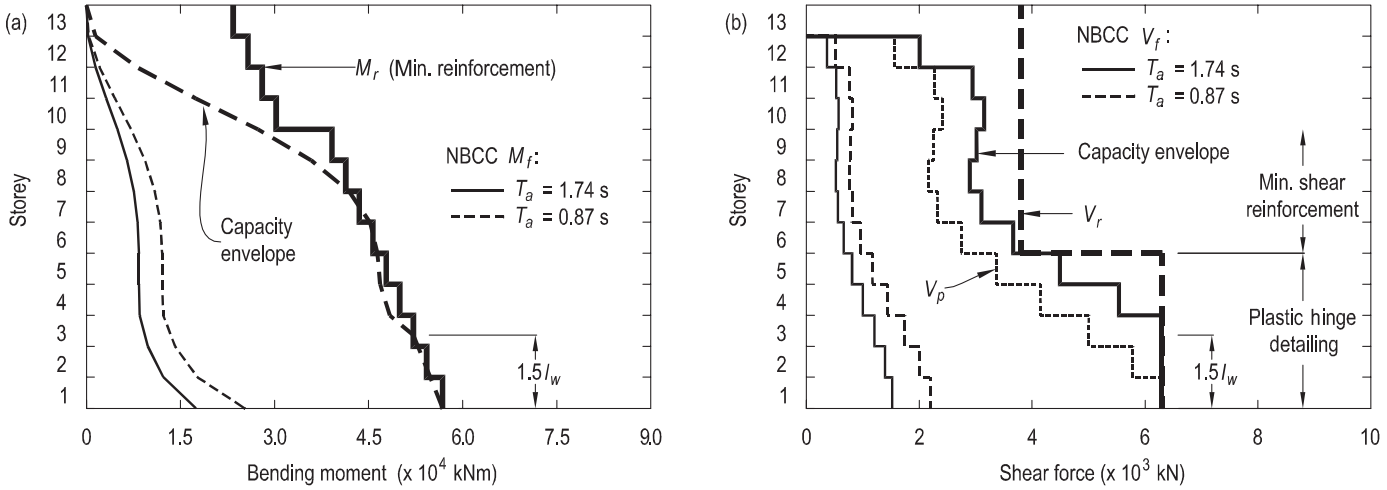

the CSA standard A23.3-04 does not specify any upper limit for γ_w, only a lower limit of 1.3.

As shown in Fig. 4, for the north–south direction, the substantial flexural overstrength of the core wall at the base produces a significantly large design shear envelope V_p for the walls, as compared with V_f. In the north–south direction, V_p at the wall base is approximately equal to the maximum factored shear resistance ($V_{r,max}$) allowed by CSA standard A23.3-04 for the base plastic hinge region.

As a result of the large flexural overstrength of the wall and the very low design overall drifts of the building, the calculated inelastic rotational demands, θ_{id}, on the structural components of each wall system are very low, particularly for the walls, compared with the inelastic rotational capacities, θ_{ic}, specified by CSA standard A23.3-04 for these components. Although the ductility requirement is satisfied ($\theta_{id} < \theta_{ic}$), the anticipated inelastic deformation level of the core wall is not in line with that assumed for design ($R_d > 3.0$).

The previous design issues indicate that excessive flexural overstrength can inhibit the intended large inelastic deformation of ductile RC walls under strong ground motions and hence the intended earthquake load reduction on the structure.

4. Modeling for inelastic analysis

4.1. Inelastic structural models

The seismic performance of the core wall was assessed from two-dimensional (2D) inelastic static (pushover) and time-history dynamic analyses using two finite-element structural analysis programs, namely RUAUMOKO (Carr 2002) and EFiCoS (Légeron et al. 2005). RUAUMOKO mainly uses lumped plasticity beam elements to represent RC members, and EFiCoS uses layered beam elements with uniaxial constitutive laws based on the continuum damage mechanics for concrete and the plasticity theory for steel. EFiCoS was used primarily to validate RUAUMOKO models (Boivin 2006).

The wall system in each principal direction was modeled as an isolated wall fully fixed at its base. This results in a cantilever wall model for the north–south direction and a coupled wall model for the east–west direction. The walls and coupling beams were modeled with beam-line finite elements, which are located at member centroids. The end regions of the coupling beams were represented with rigid end extensions to account for the finite widths of the adjoining walls. Figure 5 shows the 2D RUAUMOKO wall mod-

Fig. 5. RUAUMOKO structural models for inelastic seismic analysis. (M_y, yield moment; M_{cr}, cracking moment; φ, curvature).

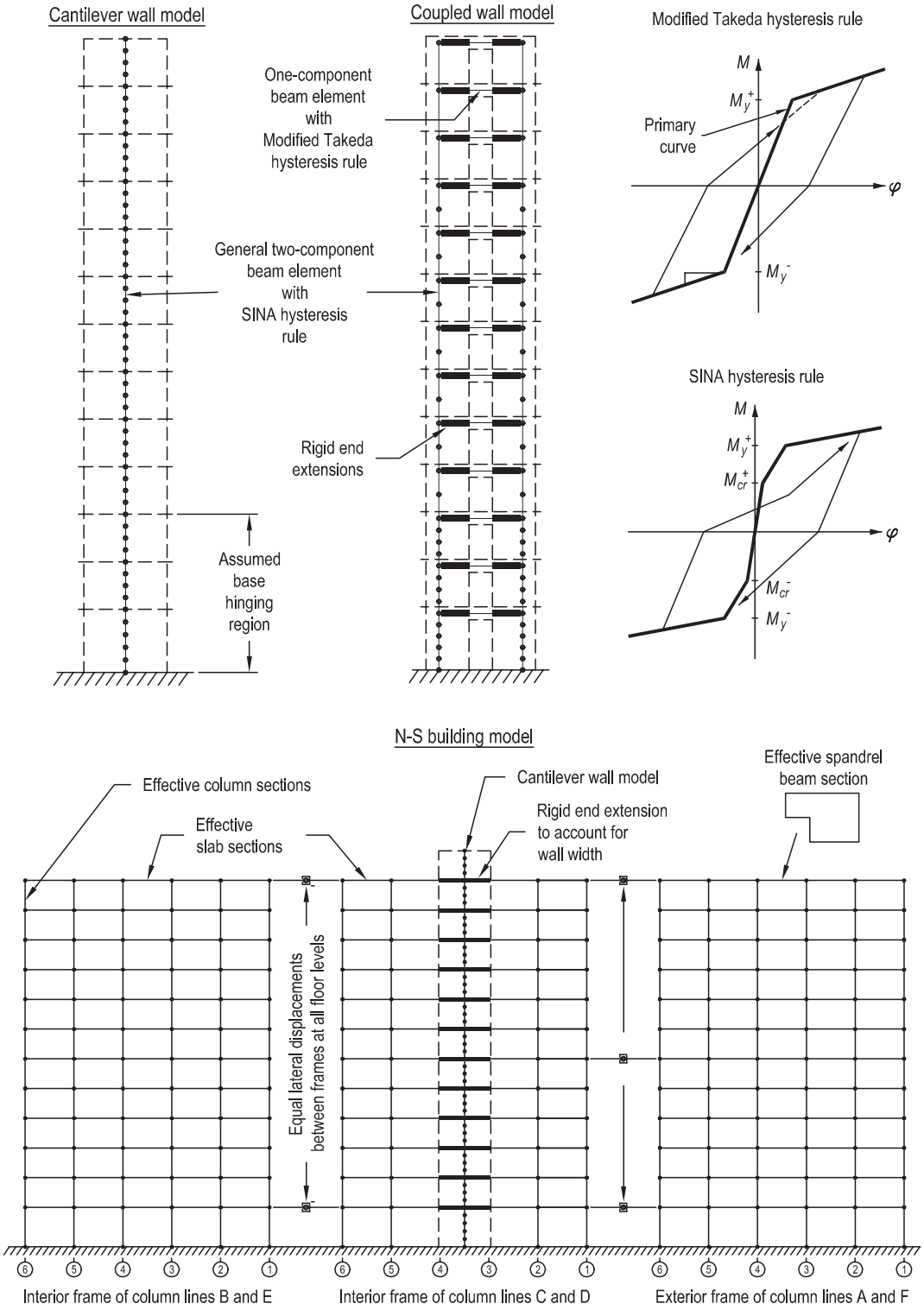

els developed for analysis and the modeling parameters adopted to simulate the inelastic behavior in flexure of the structural members. Shear deformation was assumed to be linearly elastic, given the use of capacity design principles for shear strength design. The elastic shear stiffness of members was based on their effective shear area. As members were modeled with lumped plasticity elements, the modified bilinear Takeda hysteresis rule was used for coupling beams, and the trilinear SINA hysteresis rule was used for walls. The latter rule makes it possible to capture the uncracked elastic response, which is significant for the wall under study, and to account for the effect of the tension stiffening of the concrete on the elastic response. The influence of tension stiffening on the dynamic responses of the wall models

Table 3. Characteristics of the 2% in 50 years UHS-compatible simulated and historical ground motions for Montréal.

Earthquake time history	UHS compatibility	Trial No.	Scaling factor	PGA (g)	t_D (s)
Simulated record					
M 6.0 events at R = 30 km for eastern Canadian sites (Atkinson 1999)	Scaled in time domain to match design (median) UHS	1	0.85	0.37	6.6
		2	0.85	0.44	6.5
		3	0.85	0.40	6.5
M 7.0 events at R = 70 km for eastern Canadian sites (Atkinson 1999)	Scaled in time domain to match design (median) UHS	1	0.90	0.27	20.8
		2	0.90	0.26	20.7
		3	0.90	0.31	21.0
Historical record					
1988 M 5.9 Saguenay, Chicoutimi-Nord station, R = 43 km, component 124°	Original (not scaled)	—	—	0.13	17.6
	Scaled in frequency domain to match design (median) UHS	—	—	0.43	16.1
	Scaled in frequency domain to match 84th percentile UHS	—	—	0.63	17.9
1940 M 6.9 Imperial Valley, El Centro station, R = 12 km, N–S component	Original (not scaled)	—	—	0.35	24.4
	Scaled in frequency domain to match design (median) UHS	—	—	0.43	23.8
	Scaled in frequency domain to match 84th percentile UHS	—	—	0.63	24.3

Note: M, moment magnitude; PGA, peak ground acceleration; R, epicentral distance; t_D, Trifunac duration (time interval during which 5%–95% of the total ground shaking energy is delivered).

was investigated (Boivin 2006). It was observed, primarily for lumped plasticity modeling, that not taking into account tension stiffening can lead to considerable underestimation of the wall shear demand when the wall structure behavior in flexure is lightly inelastic. The concrete tension-stiffening effect then was accounted for through the trilinear moment–curvature relationships determined for each storey from the sectional analysis program MNPhi (Paultre 2001). The strain hardening of steel was also taken into account. An elastic – perfectly plastic relationship was used as a primary curve for the modified Takeda rule. Strength decay was not accounted for in the structural models. Note that the bending yield strength, M_y, used for the hysteresis rules is the code-specified flexural strength of the member section. It was determined for a factored, nominal, and probable resistance, as defined in CSA standard A23.3-04.

The wall models assumed that the building floors act as rigid diaphragms. Consequently, the mass of each storey was lumped at each floor level of the wall models. The total mass of the penthouse was lumped at the building roof. The seismic weight of the building used for analysis corresponded to the 2005 NBCC seismic loading case with 100% of dead loads, 50% of live loads, and 25% of snow load.

As shown in Fig. 5, a 2D inelastic structural model of the entire building structure in the north–south direction was also considered for analysis to assess the influence on the wall system of the added stiffness from structural components not part of the SFRS. A previous study (Renaud 2004) on a similar core wall building suggested that this influence is negligible in the coupled wall direction because of the larger lateral stiffness of the SFRS, induced by the large coupling action, over the entire height of the building.

4.2. Earthquake ground motion histories

A suite of two historical and six simulated ground motion time histories was used for the inelastic time-history dynamic analysis. Table 3 gives the characteristics of these time histories, and Fig. 6 illustrates their time history. Two excitation levels were considered: one corresponding to the design (median 2% in 50 years) UHS for Montréal, and another corresponding to the 84th percentile 2% in 50 years UHS for Montréal. The simulated time histories are design UHS-compatible accelerograms (Fig. 7*a*), as required by the 2005 NBCC for seismic design, and are representative of ground motions for magnitude–distance scenarios that dominate the seismic hazard of Montréal for the design probability level. The historical records were scaled in the frequency domain with the program SYNTH (Naumoski 2001) through an iterative suppression-raising technique to match the design and the 84th percentile 2% in 50 years UHS for Montréal over the entire period range of interest, as shown in Fig. 7*b*. Although spectrum-compatible accelerograms are unrealistic and physically inconsistent, various works (Léger et al. 1993) suggest that the use of such accelerograms for performance assessment purposes should not affect the validity of results as long as more than one accelerogram is used.

Note that the original 1940 El Centro record was also used as input motion. The 5% damped spectral acceleration response of this record has the particularity of fairly matching the 84th percentile UHS for Montréal over the long-

Fig. 6. Time histories of typical selected ground motions.

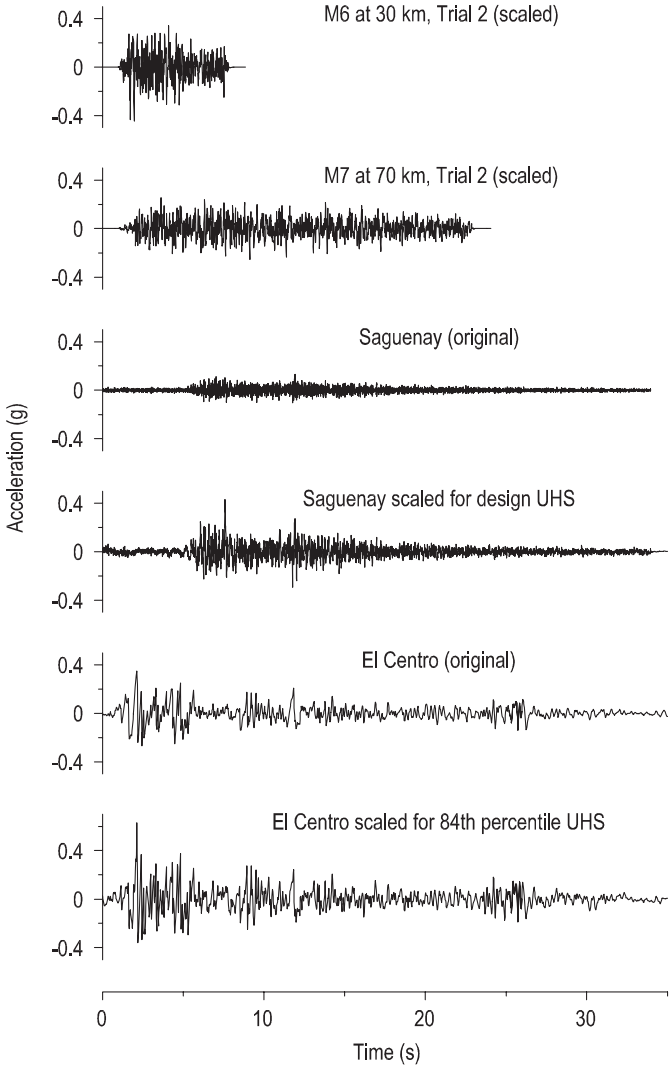

Fig. 7. The 5%-damped acceleration response spectra of selected ground motions for Montréal: (*a*) simulated records; (*b*) historical records.

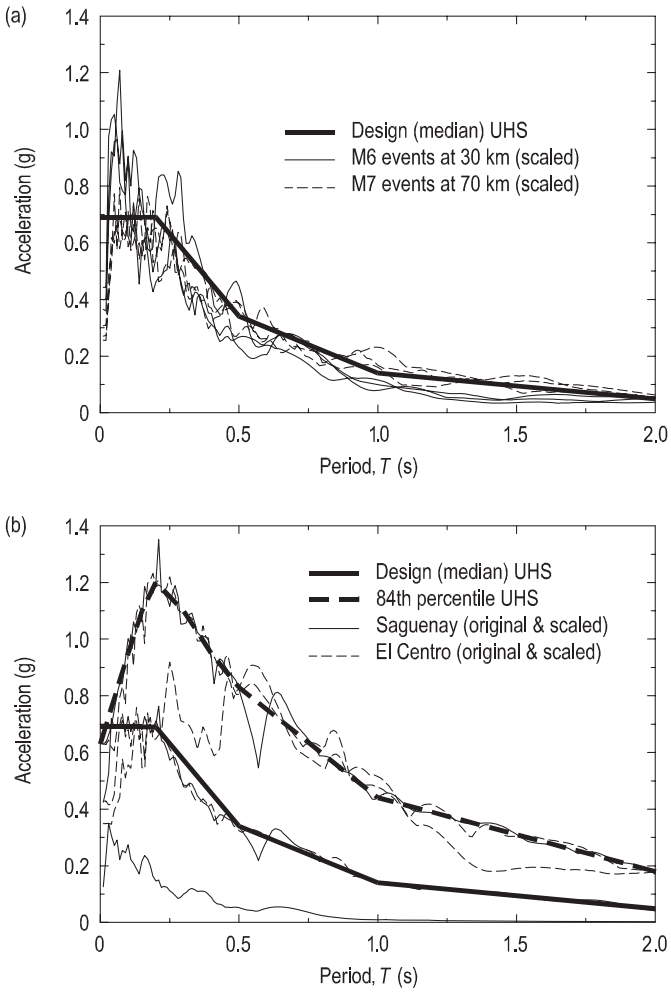

period range (>0.5 s), as shown in Fig. 7*b*, but being lower over the short-period range. This means that, theoretically, the higher mode contribution under this record should be significantly less than those under a record matching the entire 84th percentile UHS.

4.3. Damping model

Damping is one of the main unknowns in dynamic analysis. Both the damping model and the damping level used for analysis have a strong influence on predictions. Consequently, two different viscous damping models were used for the inelastic time-history analysis, namely the constant damping (CD) and the Rayleigh damping (RD) models, both based on the initial elastic stiffness of the analyzed structural model. Two damping levels were considered for the constant damping model, namely 1% and 2% of critical. These values bound the range of typical modal damping values measured in actual undamaged midrise RC wall buildings (Boroschek and Yáñez 2000). The resulting CD models are referred to as the 1% CD and 2% CD models. For the Rayleigh damping model, referred to as the 2% RD model, a modal damping ratio of 2% of critical was used for the 1st and 12th lateral vibration modes. This Rayleigh damping ensures that the modal damping ratios associated with all elastic vibration modes of the analyzed structural model are mostly within the range of 1%–2% of critical. In addition, this damping model should not produce any problems of force equilibrium due to high damping in the high modes. Note that inelastic behavior adds hysteretic damping to the initial damping.

5. Inelastic seismic analysis results

The seismic performance of the core wall was assessed from inelastic adaptive pushover and time-history dynamic analyses. Only results obtained from the dynamic analysis are presented in this paper. Those obtained from the pushover analysis can be found in Boivin (2006). These results confirm the intended inelastic mechanism of each wall system at the anticipated lateral drifts and the large flexural overstrength of the core wall. Due to this overstrength, they predict little inelastic flexural behavior of the wall at design drifts and therefore a much better performance level than that corresponding to the performance level "extensive damage," which is the level expected by the 2005 NBCC for the

2% in 50 years seismic design event and is associated with inelastic deformation at or near SFRS capacity.

The dynamic analysis was performed for probable resistance only. It was carried out using the implicit Newmark constant average acceleration integration method with a constant time step of 0.001 s and using a Newton–Raphson iteration within each time step. *P*-delta effects were not considered because they were found to be negligible for the studied structure. This is typical for walls for which higher modes control their seismic response (Tremblay et al. 2001).

The dynamic analysis results given in this section are only for a few engineering demand parameters (EDPs). The selected EDPs are wall bending moment, curvature ductility, drifts, and wall shear force. Figure 8 shows the predicted interstorey drift and wall force demands. These demands are presented as follows: (*i*) mean (M) plus or minus one standard deviation (SD) peak response (PR) to selected design UHS-compatible simulated and historical records for Montréal; (*ii*) mean peak response (MPR) to selected 84th percentile (84th) UHS-compatible historical records for Montréal; and (*iii*) MPR to the selected original El Centro (OEC) record. The means and standard deviations include the peak responses computed with the 1% CD, 2% CD, and 2% RD damping models. In Fig. 8, the predicted demands are compared with the design envelopes. Note that the design envelopes do not include any torsional effects because only 2D analysis is considered herein. The design interstorey drift envelopes were determined from 2005 NBCC requirements, using an SRSS combination, and the design force envelopes are the capacity design strength envelopes determined from CSA standard A23.3-04 and its explanatory notes (CAC 2006*a*). For comparison purposes, the CSA design moment envelope is presented in Fig. 8*b* for a probable resistance, though it is based on a factored resistance in the code. The linear moment envelope suggested in CAC (1995) is also shown in Fig. 8*b*. The CSA design shear envelope shown in Fig. 8*c* does not include the dynamic magnification due to inelastic effects of higher modes. Note that this envelope is governed by V_p over the assumed base hinging region and by the shear envelope determined in accordance with the new CSA shear strength requirement for all elevations above that of the hinging region.

5.1. Overall behavior and flexural demand

For either seismic loading direction, little flexural yielding is predicted in the core wall when subjected to design-level ground motions, and substantial yielding, without exceeding the ultimate flexural capacity, is predicted when subjected to 84th-level and OEC ground motions.

For north–south seismic loading, the simulations with the cantilever wall model generally predict a plastic hinge at the wall base and, in some cases, a few additional hinges at the middle and upper storeys for the design-level, 84th-level, and OEC excitations, as indicated in Table 4 for a 2% RD (note that similar predictions are obtained with the 1% and 2% CDs). The same simulations conducted with EFiCoS do not predict any yielding above the assumed base hinging region for a design-level excitation but do predict the onset of yielding in the outermost reinforcing bars at midstorey for the above-design-level excitations, as shown in Fig. 9. Based on this figure, no concrete damage in compression is predicted even at the 84th-level excitation, but tensile cracking over a large part of the wall is predicted. Based on EFiCoS predictions, it appears that the hinges at the middle and upper storeys predicted by the RUAUMOKO cantilever wall model are more a modeling issue than a design issue related to lumped plasticity modeling. This statement is reinforced by the flexural predictions obtained with the RUAUMOKO model of the north–south building, where the inelastic action in the wall is constrained at its base for the three levels of excitation, as indicated in Table 4. This suggests that the modeling approach adopted and the added stiffness from structural components not part of the SFRS may have a strong influence on hinge formation predictions for multistorey cantilever walls. Nevertheless, the previous predictions indicate that the capacity design moment envelope determined from the new CSA standard A23.3-04 provision has prevented the formation of unintended plastic hinges, even for an excitation level significantly above that of the design level. Actually, Fig. 8*b* shows that, in general, the CSA design envelope conservatively estimates the predicted wall moment demands for the three levels of excitation. Figure 8*b* also shows that the linear probable envelope suggested in CAC (1995) underestimates the predicted demands at the middle and upper storeys. This shows once more that this envelope is inadequate to capture the higher mode contribution in the flexural response.

For east–west seismic loading, the simulations with the coupled wall model predict hinging solely at beam ends when subjected to design-level motions and at both beam ends and wall base when subjected to 84th-level and OEC motions. Even under the above-design-level motions, the mean beam curvature ductility demand remains lower than the ultimate curvature ductility, which corresponds to the inelastic rotational capacity of 0.04 rad specified in CSA standard A23.3-04 for diagonally reinforced coupling beams. Figure 8*b* shows that the predicted wall moment demands are conservatively estimated by the 2004 CSA design envelope (which was determined for the compression wall), except when a wall acts as a tension wall under the 84th-level and OEC excitations. In these cases, the predicted flexural demand at upper storeys exceeds that of the design envelope.

It is of interest to note that the RUAUMOKO model of the complete north–south building predicts plastic hinges only in the wall system when subjected to the design-level motions. Additional plastic hinges are predicted mainly in the base columns of all frames and the spandrel beams of the exterior frame when subjected to above-design-level motions.

5.2. Overall and interstorey drifts

Figure 8*a* shows that, for either seismic loading direction, the interstorey drift demands predicted with the design-level motions are less than or equal to 0.5%, and those predicted with the 84th-level and OEC motions range between 0.5% and 1.5%. These values are largely less than the NBCC limit of 2.5% for the studied building. Although not shown, the mean predicted overall drift demands are less than 0.3% and 0.7% for the design-level and above-design-level motions, respectively. Figure 8*a* shows that the NBCC design envelope for the cantilever wall direction underestimates the predicted drift demand when the structure is subjected to design-level motions. For both directions, the design enve-

Fig. 8. Inelastic time-history dynamic analysis results obtained from RUAUMOKO structural models: (*a*) drift; (*b*) flexure; (*c*) shear.

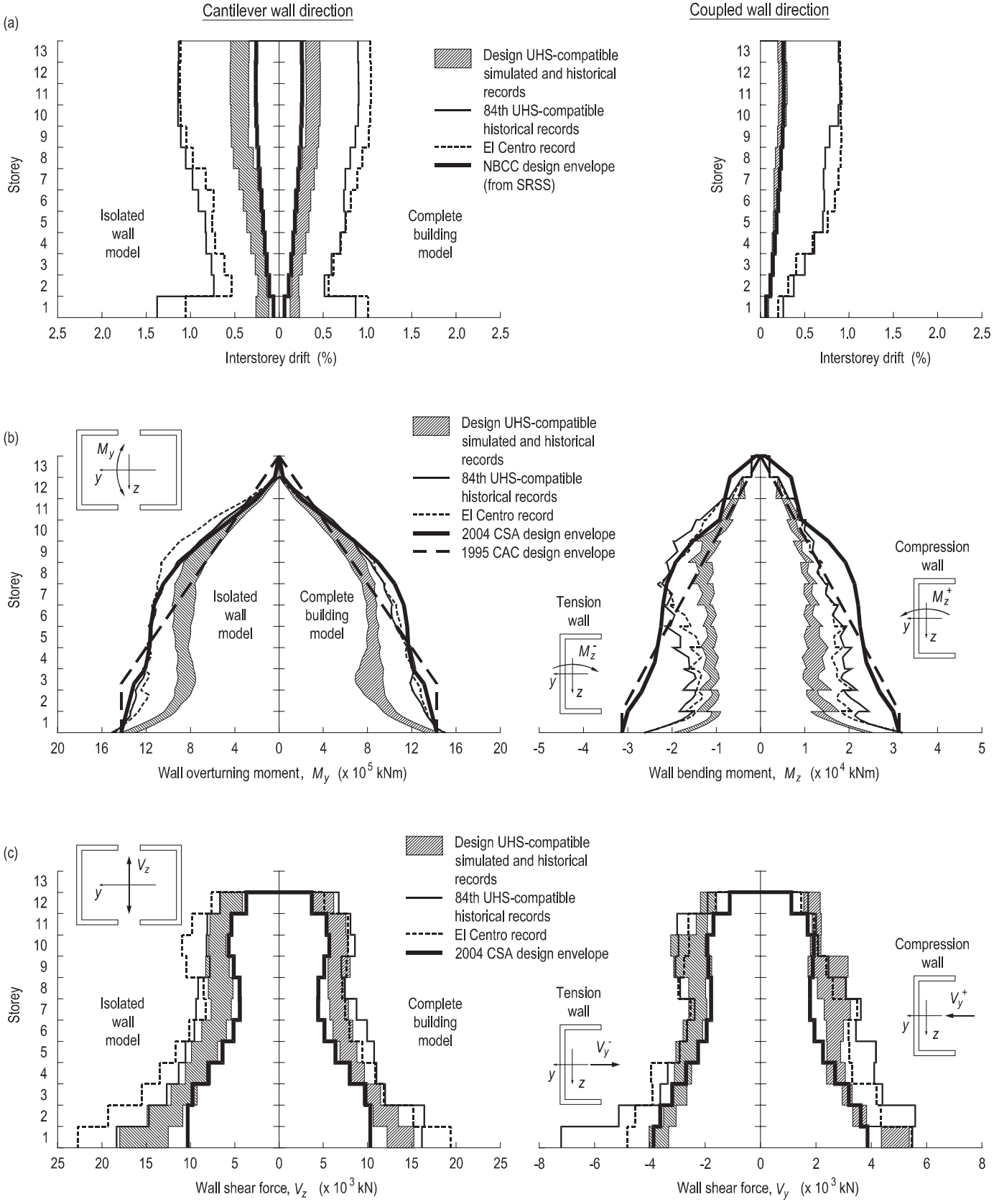

Table 4. Predicted plastic hinges in wall systems for Rayleigh damping with 2% in 1st and 12th lateral vibration modes (2% RD).

Structural model	Design UHS-compatible records							84th UHS-compatible records					
	M6@30km		M7@70km		Saguenay		El Centro	Saguenay		El Centro		El Centro (original)	
	Location	μ_ϕ	Location	μ_ϕ	Location	μ_ϕ	Location	μ_ϕ	Location	μ_ϕ	Location	μ_ϕ	Location	μ_ϕ
Cantilever wall	None	—	Base	1.3	Base	1.2	Base	1.4	Base	12	Base	7.3	Base	9.8
			S8	3.4					S6	1.7			S8	1.8
									S7	4.0			S9	1.1
North-South building	Base	1.3	Base	1.4	None	—	Base	1.3	Base	7.8	Base	8.0	Base	10
Coupled wall	Beams	2.5	Beams	2.4	Beams	2.9	Beams	1.8	Beams	7.0	Beams	8.0	Beams	7.6
									Walls[a]	3.0	Walls[a]	2.3	Walls[a]	2.0

Note: S6–S9 denote storey level (with S1 as the base up to S13 as the penthouse). μ_ϕ, curvature ductility.

[a]Base of walls.

lopes significantly underestimate the drift demands predicted with the above-design-level motions. Obviously any large drifts resulting from local yielding cannot be captured by the NBCC envelopes, since they were determined from linear analysis.

5.3. Shear demand

For either seismic loading direction, Fig. 8*c* shows that the wall shear force demand predicted with the design-level motions significantly exceeds that of the CSA design envelope, and hence V_p, though the shape of both the demand and the envelope over the wall height is almost the same. Figure 8*c* also shows that the wall shear predictions obtained with the cantilever wall model and the north–south building model are very similar, though slightly less with the building model. This means that the added stiffness from structural components not part of the SFRS has a negligible effect on the wall shear predictions. From Fig. 8*c*, it is noted that the OEC motion produces a larger base shear demand on the cantilever wall than that of the 84th-level motions, even though its high-frequency acceleration content is much less significant, as illustrated in Fig. 7. An opposite result, however, is observed in Fig. 8*c* for the coupled wall direction, particularly when the wall acts as a tension wall. These observations suggest that spectrum-compatible motions may not represent conservative input, unlike commonly assumed, for wall shear predictions.

The ratio of the predicted wall shear force demand to the CSA design shear envelope at each storey is defined as the dynamic shear magnification factor β_V. Tables 5 and 6 give this factor for the cantilever and coupled wall systems, respectively. In these tables, the β_V value at the wall base and the average value over all storeys (AOS) are given for the MPR and M + SD PR to design-level motions and the MPRs to OEC and 84th-level motions. These tables show that, for the M + SD demand predicted from the design-level motions, the base and AOS β_V values are about 1.5 for the cantilever system and about 1.4 and 1.5 for the coupled wall system. The β_V values are not larger than 1.9 for the above-design-level excitations. For comparison purposes, the value of the New Zealand dynamic shear magnification factor, ω_v, for the studied building is 1.7.

6. Discussion

Based on the analysis results presented previously, the overall seismic performance in flexure to be expected for the core wall structure under possible design-level ground motions is much better than that of the performance level "extensive damage" (equivalent to "near collapse" in the Structural Engineers Association of California Vision 2000 committee document (SEAOC 1995)) expected by the 2005 NBCC for the 2% in 50 years seismic design event. Actually, as damage increases with increasing inelastic lateral deformation, the low level of inelastic action predicted in the wall structure for the design-level excitation indicates that the structure should be slightly damaged. Even for the 84th-level and OEC excitations, the predicted lateral deformation demand on the structure is less than the deformation capacity. This better than expected performance is mainly due to the large flexural overstrength resulting from the ex-

Fig. 9. Damage predicted by EFiCoS in cantilever wall system under 84th-level Saguenay motion for a 2%-RD: (*a*) concrete damage in compression (*b*) concrete damage in tension (*c*) plasticity in steel rebars (Concrete damage: blue (dark grey in print version) = 0%; red (light grey in print version) = 100%; Rebar plasticity: blue = no; red = yes).

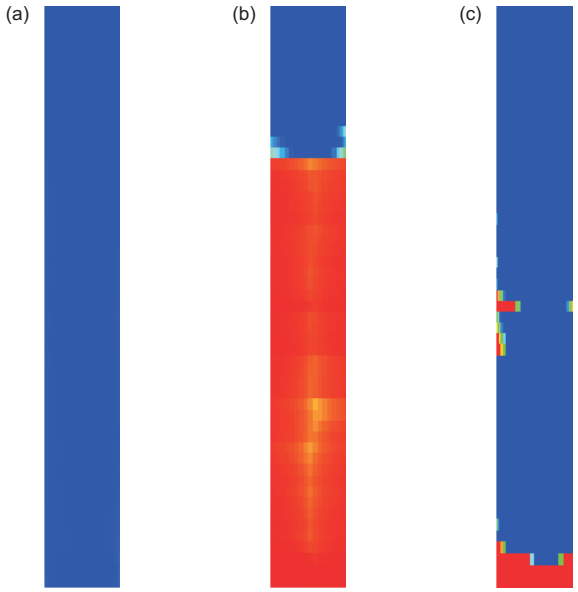

cess strength at the wall base arising from the required minimum reinforcement. This excess strength then inhibits the intended large inelastic deformation of the ductile wall structure under the design earthquake and the intended force reduction assumed for design. This means that excess strength in flexure should be avoided as much as possible in the assumed base hinging region of a ductile wall.

It is important to add that the predicted good flexural performance of the studied structure is also due to adequate prevention of unintended plastic hinge formation in the walls. This suggests that the new capacity design method of CSA standard A23.3-04 for the flexural strength design of ductile walls is adequate to constrain the inelastic mechanism of the walls at their intended base hinging region. Note that coupling beams provide an additional inelastic mechanism in ductile coupled wall systems.

Despite the predicted good flexural performance of the wall structure, the predicted shear demand for the design-level excitation significantly exceeds the CSA design shear envelope. This suggests a potential shear failure, which would prevent the wall structure from laterally deforming in a ductile manner. In such cases, the seismic performance of the structure might be closer to "extensive damage" than what is predicted in flexure. This scenario is not so unrealistic because the current predictions do not account for shear increase due to torsional effects.

One could explain the exceeding shear predictions for the design-level excitation by the linear shear assumption used to model the shear behavior of the wall structure. Laboratory tests (Oesterle et al. 1977) showed that flexural yielding at the base hinging region of a wall triggers shear yielding behavior, even if shear strength design is based on capacity design principles. Another explanation could be the dynamic magnification due to inelastic effects of higher vibration modes, since the CSA design envelope does not account for this magnification, which should increase with ductility demand as the relative contribution of higher modes increases (Seneviratna and Krawinkler 1994; Priestley 2003). Actually, based on Tables 5 and 6, scaling up the CSA design envelope with the dynamic shear magnification factor ω_v of 1.7 for the studied building produces much better wall shear estimates for motions at design level and even above. However, none of the previous explanations stand up because very little inelastic action, and hence ductility demand, is predicted in the wall structure for the design-level excitation.

Table 5. Dynamic shear magnification factor, β_v, for cantilever wall system (from building model).

	Design UHS-compatible records		84th UHS-compatible records	Original El Centro record
	(MPR)	(M + SD)	(MPR)	(MPR)
AOS	1.29	1.47	1.60	1.49
Base	1.33	1.48	1.57	1.88

Table 6. Dynamic shear magnification factor, β_v, for coupled wall system (maximum of both tension and compression walls).

	Design UHS-compatible records		84th UHS-compatible records	Original El Centro records
	(MPR)	(M + SD)	(MPR)	(MPR)
AOS	1.28	1.48	1.69	1.49
Base	1.26	1.39	1.86	1.41

Figure 10 illustrates a reason for the exceeding shear demand under the design-level excitation. Actually, the predictions obtained from the inelastic dynamic analysis are based on realistic 1%–2% damping ratios, whereas the CSA design shear envelope is based on the common 5% damping, as it was obtained by scaling up the NBCC design shear envelope determined from the response spectrum method. This damping overestimation produces a significant underestimation of the higher mode contribution in the NBCC design forces due to lower spectral accelerations ($S_a(T)$), as illustrated in Fig. 10. As a result, the CSA design envelope underestimates the predicted wall shear demand, even though the wall response is almost elastic under the design-level excitation. The use of 5% damping for the inelastic dynamic analysis would have hidden the shear underestimation problem for the design-level excitation, as shown in Fig. 11. Of course, the CSA design shear envelope will underestimate any excitations above design level, as shown in Fig. 11, because shear demand, including inelastic dynamic magnification effects, increases with an increase in ground motion intensity (Amaris 2002). The previous observations suggest then that the 5% damped spectral accelerations ($S_a(T)$) prescribed by the 2005 NBCC for seismic design can underestimate the higher mode responses of walls sensitive to higher mode effects and, as a result, that the capacity design method prescribed by CSA standard A23.3-04 may be inadequate for

Fig. 10. Mean and simplified acceleration response spectra obtained from all selected simulated records for Montréal. $T_1 - T_3$, 1st–3rd lateral vibration periods of the studied building.

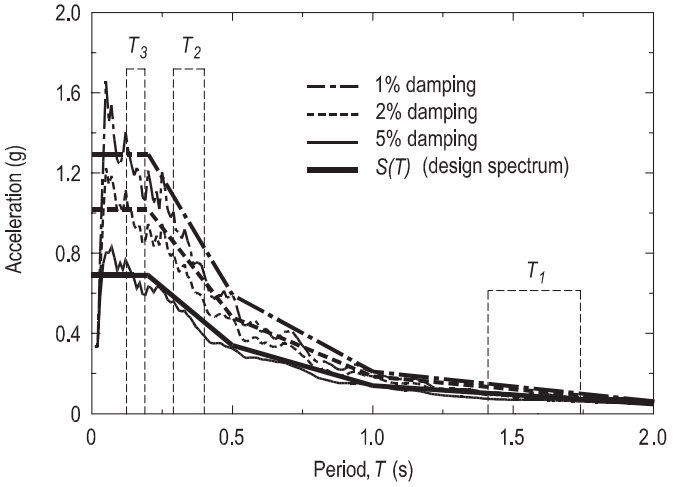

Fig. 11. Shear responses of the cantilever wall model for 5% damping.

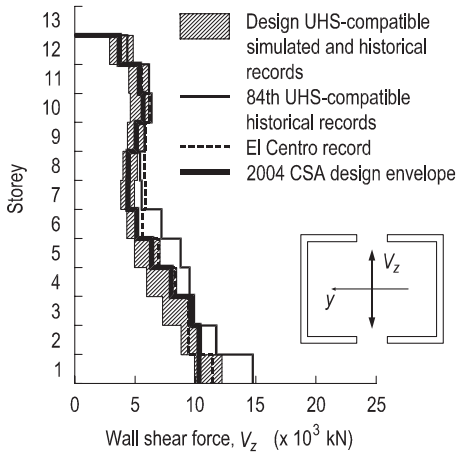

estimating the shear demand on such walls, even when their behavior is lightly inelastic.

To verify this statement, simplified acceleration response spectra similar to the NBCC design spectrum were determined, for 1% and 2% damping, from the mean response spectra of all selected simulated records for Montréal, as shown in Fig. 10. Although not shown, these simplified spectra lie between the mean and the M + SD design spectra proposed by Atkinson and Pierre (2004) for 1% and 2% damping. Using the simplified spectra as input in the linear response spectrum method, new NBCC and CSA seismic design envelopes were determined for 1% and 2% damping. Although they are not shown in this paper, these envelopes are very good or conservative estimates of the demands predicted from the inelastic time-history analysis for design-level motions and the same damping values. The new CSA design shear envelope for the walls, however, matches fairly well or underestimates the M – SD demand predicted from the inelastic time-history analysis, particularly in the cantilever wall direction. Table 7 gives the probable base shear (V_p) for the cantilever wall system determined from $S_a(T)$ values based on 1%, 2%, and 5% (code value) damping. Table 7 indicates that, as V_f (and M_f) considerably increases with decreasing damping, γ_p decreases, given that M_p at the wall base remains constant. This results in V_p increasing by only 6% and 16% as damping drops from 5% to 2% and 1%, respectively. Based on Table 5, these increases are not enough to adequately estimate the predicted shear demand on the cantilever wall system. This shows a deficiency of eq. [3] to suitably estimate the shear demand on walls whose seismic response is dominated by higher modes, even though this response is almost elastic. This deficiency reinforces the need for CSA standard A23.3-04 to provide an adequate capacity design method, taking into account the inelastic magnification effects of higher modes, for the shear strength design of ductile RC walls.

Table 7. Probable base shear (eq. [3]) for the cantilever wall system determined from $S_a(T)$ based on 1%, 2%, and 5% (design) equivalent viscous damping (no torsional effects).

Damping for $S_a(T)$ (%)	γ_p	V_f (kN)	V_p (kN)	$V_p/V_p^{5\%}$
5	5.00	2062	10 300	—
2	3.71	2937	10 915	1.06
1	3.24	3691	11 972	1.16

7. Conclusion

In this work, a 12-storey ductile concrete core wall located in Montréal was designed according to the 2005 edition of the *National building code of Canada* (NBCC) and the 2004 Canadian Standards Association (CSA) standard A23.3-04 for seismic loading and analyzed in the nonlinear regime. The analysis results obtained in this work indicate that the overall seismic performance in flexure to be expected for the core wall structure under possible design-level ground motions is much better than that of the performance level "extensive damage" expected by the 2005 NBCC for the 2% in 50 years seismic design event. However, there is a risk of shear failure of wall members due to an underestimation at the design stage of the seismic wall shear demand.

This work suggests the following main conclusions with regard to seismic design with the 2005 NBCC and CSA standard A23.3-04 for midrise ductile RC shear walls:

(1) Unlike the linear probable moment method suggested in CAC (1995), the new method prescribed by CSA standard A23.3-04 for determining the capacity design moment envelope for ductile walls may provide conservative estimates and hence may prevent unintended plastic hinge formation.

(2) The 5% damped spectral accelerations ($S_a(T)$) prescribed by the 2005 NBCC underestimate the higher mode responses of walls whose seismic response is dominated by higher modes.

(3) The shear strength requirements prescribed by CSA standard A23.3-04 can produce capacity design shear envelopes that significantly underestimate the shear demand on such walls, even when the wall behavior is slightly inelastic and the NBCC design forces are determined

from $S_a(T)$ values based on realistic damping values for these walls. This suggests that the new design codes may be inadequate to prevent a shear failure in such walls under a design earthquake.

(4) A capacity design method for shear strength design is required for CSA standard A23.3-04. Meanwhile, scaling up the CSA design shear envelope by the New Zealand dynamic shear magnification factor ω_v seems to be a reasonable approach for estimating wall shear demand.

As this work is based on two-dimensional (2D) simulations of a single typical RC core wall structure that, moreover, has substantial flexural overstrength, more analysis is needed to reinforce the previous conclusions.

Acknowledgements

The authors gratefully acknowledge the financial support of the Natural Sciences and Engineering Research Council of Canada under the Discovery Grant and the Strategic Research Networks program and of the Fonds de recherche sur la nature et les technologies du Québec under the Regroupements stratégique program.

References

Amaris, A.D.M. 2002. Dynamic amplification of seismic moments and shear forces in cantilever walls. M.Sc. thesis, European School of Advanced Studies in Reduction of Seismic Risk (ROSE), Pavia, Italy.

Atkinson, G. 1999. Spectrum-compatible time histories for 1/2500 P.A. uniform hazard spectra of Adams et al. (1999). Discussion note.

Atkinson, G.M., and Pierre, J.-R. 2004. Ground-motion response spectra in eastern North America for different critical damping values. Seismological Research Letters, **75**(4): 541–545. doi:10.1785/gssrl.75.4.541.

Bachmann, H., and Linde, P. 1995. Dynamic ductility demand and capacity design of earthquake-resistant reinforced concrete walls. *In* Recent Developments in Lateral Force Transfer in Buildings: Proceedings of the Tom Paulay Symposium, La Jolla, Calif. *Edited by* N. Priestley, M.P. Collins, and F. Siable. ACI Special Publication SP-157, American Concrete Institute (ACI), Farmington Hills, Mich. pp. 117–139.

Blakeley, R.W.G., Cooney, R.C., and Megget, L.M. 1975. Seismic shear loading at flexural capacity in cantilever wall structures. Bulletin of the New Zealand National Society for Earthquake Engineering, **8**(4): 278–290.

Boivin, Y. 2006. Assessment of the seismic performance of a 12-storey ductile concrete shear wall system designed according to the NBCC 2005 and the CSA A23.3 2004 standard. M.Sc. thesis, Université de Sherbrooke, Sherbrooke, Que.

Boroschek, R.L., and Yáñez, F.V. 2000. Experimental verification of basic analytical assumptions used in the analysis of structural wall buildings. Engineering Structures, **22**(6): 657–669. doi:10.1016/S0141-0296(99)00007-3.

CAC. 1995. Explanatory notes on CSA standard A23.3-94. Cement Association of Canada (CAC), Ottawa, Ont.

CAC. 2006*a*. Explanatory notes on CSA standard A23.3-04. Cement Association of Canada (CAC), Ottawa, Ont.

CAC. 2006*b*. Concrete design handbook. 3rd ed. Cement Association of Canada (CAC), Ottawa, Ont.

Carr, A.J. 2002. Computer program RUAUMOKO. Department of Civil Engineering, University of Canterbury, Christchurch, New Zealand.

Chaallal, O., and Gauthier, D. 2000. Seismic shear demand on wall segments of ductile coupled shear walls. Canadian Journal of Civil Engineering, **27**(3): 506–522. doi:10.1139/cjce-27-3-506.

CSA. 1994. Design of concrete structures. CSA standard A23.3-94, Canadian Standards Association (CSA), Toronto, Ont.

CSA. 2004. Design of concrete structures. CSA standard A23.3-04, Canadian Standards Association (CSA), Toronto, Ont.

Eberhard, M.O., and Sozen, M.A. 1993. Behavior-based method to determine design shear in earthquake-resistant walls. Journal of Structural Engineering, ASCE, **119**(2): 619–640. doi:10.1061/(ASCE)0733-9445(1993)119:2(619).

Humar, J., and Mahgoub, M.A. 2003. Determination of seismic design forces by equivalent static load method. Canadian Journal of Civil Engineering, **30**(2): 287–307. doi:10.1139/l02-067.

Léger, P., Tayebi, A.K., and Paultre, P. 1993. Spectrum-compatible accelerograms for inelastic seismic analysis of short-period structures located in eastern Canada. Canadian Journal of Civil Engineering, **20**(6): 951–968.

Légeron, F., Paultre, P., and Mazars, J. 2005. Damage mechanics modeling of nonlinear seismic behavior of concrete structures. Journal of Structural Engineering, ASCE, **131**(6): 946–955. doi:10.1061/(ASCE)0733-9445(2005)131:6(946).

Naumoski, N.D. 2001 Program SYNTH — generation of artificial accelerograms compatible with a target spectrum. Department of Civil Engineering, University of Ottawa, Ottawa, Ont.

NRCC. 1995. National Building Code of Canada. Part 4: Structural design. Canadian Commission on Building and Fire Codes, National Research Council of Canada (NRCC), Ottawa, Ont.

NRCC. 2005. National Building Code of Canada. Part 4: Structural design. Canadian Commission on Building and Fire Codes, National Research Council of Canada (NRCC), Ottawa, Ont.

NZS. 1995. Concrete structures standard. Part 1: the design of concrete structures. Part 2: commentary on the design of concrete structures. NZS 3101, Standards New Zealand, Wellington, New Zealand.

Oesterle, R.G., Aristizabal, J.D., Fiorato, A.E., Russell, H.G., and Corley, W.G. 1977. Earthquake-resistant structural walls — tests of isolated walls: phase II. Report to the National Science Foundation, Portland Cement Association, Skokie, Ill.

Panneton, M., Léger, P., and Tremblay, R. 2006. Inelastic analysis of a reinforced concrete shear wall building according to the National Building Code of Canada 2005. Canadian Journal of Civil Engineering, **33**(7): 854–871. doi:10.1139/L06-026.

Paultre, P. 2001. MNPHi: a program for sectional analysis of structural concrete — user manual. CRGP Report 2001-01, Department of Civil Engineering, Université de Sherbrooke, Sherbrooke, Que.

Priestley, M.J.N. 2003. Does capacity design do the job? An examination of higher mode effects in cantilever walls. Bulletin of the New Zealand Society for Earthquake Engineering, **36**(4): 276–292.

Renaud, L. 2004. Étude du comportement ductile d'un mur de cisaillement dimensionné avec un facteur de modification de force (R) de 3.5 soumis à des charges statiques et sismiques. M.Sc. thesis, Université de Sherbrooke, Sherbrooke, Que.

SEAOC. 1995. Performance based seismic engineering of buildings. Structural Engineers Association of California Vision 2000 Committee (SEAOC), Sacramento, Calif. Vol. 1.

Seneviratna, G.D.P.K., and Krawinkler, H. 1994. Strength and displacement demands for seismic design of structural walls. *In* Proceedings of the 5th US National Conference on Earthquake Engineering, Chicago, Ill., 10–14 July 1994. Earthquake Engineering Research Institute (EERI), Oakland, Calif. Vol. 2, pp. 181–190.

Tremblay, R., Léger, P., and Tu, J. 2001. Inelastic seismic response of concrete shear walls considering *P*-delta effects. Canadian Journal of Civil Engineering, **28**(4): 640–655. doi:10.1139/cjce-28-4-640.

White, T., and Ventura, C.E. 2004. Ground motion sensitivity of a Vancouver-style high rise. Canadian Journal of Civil Engineering, **31**(2): 292–307. doi:10.1139/l03-102.